Structure and Dynamics of the Polyelectrolyte Complex Formation†

Natalia V. Pogodina*,‡ and Nickolay V. Tsvetkov§

Department of Polymer Science and Engineering, University of Massachusetts at Amherst, Amherst, Massachusetts 01003 and Research Institute of Physics (Petrodvorets Branch), St. Petersburg State University ul. Ul'yanovskaya 1, Petrodvorets 198904, Russia

Received December 6, 1996; Revised Manuscript Received June 6, 1997⊗

ABSTRACT: The complex formation in the oppositely charged linear and flexible polyelectrolytes: quaternized poly(vinylpyridinium) (QPVP) and poly(sodium styrenesulfonate) (NaPSS) was investigated by static and dynamic light scattering (LS), flow birefringence (FB), and viscometry over a wide range of mixing ratios $0.003 \leq m \leq 0.9$. NaPPS/QPVP systems in *N*-methylformamide + 0.01 M KBr generated complexes with fractal geometries. The observed clusters were stable and had average dimensions $R_g \approx R_h \approx 1000$ Å at low and high mixing ratios. As the mixing ratio approached $m = 0.4$, which corresponds to the gel point, the number and the dimensions of clusters grew to $R \approx 1500-3000$ Å with a corresponding increase of the fractal parameter $d \approx 3$. According to FB data, the axial ratio of the clusters at the gel point $m = 0.4$ was $p = L/d = 1.07$, which supports a model with spherical shape.

Introduction

Interpolyelectrolyte complexes combine unique physicochemical properties with high biocompatibility. Therefore, special attention has been drawn to their application in ecology, biotechnology, and medicine.[1−6] Moreover, polyelectrolyte complexes using synthetic polyelectrolytes present convenient models for the processes that take place in biopolymers.

Significant success in the study and interpretation of the kinetics and mechanism of interpolyelectrolyte reactions, from a thermodynamical point of view, has been achieved by Kabanov.[1−4,7−14] These studies considered the influence of the polycation molar mass on the formation of water-soluble complexes in terms of the "guest−host" concept. It was found that the rate constant of the exchange reaction is independent of the polyanion chain length and increases sharply with a decrease of the polycation ionic strength.[2,10−13,14] However, a contradictory result was reported by Vishalakshi et al.[15] In that study, the molecular weight of the polycation and the location of the ionic site on the polycation did not show any effect on the complexation.

Systematic studies of various parameters influencing the structure of quasi-soluble complexes, was undertaken by Philipp[16−21] using light scattering. The concentration of polyelectrolyte solutions, degree of conversion, salt content of the medium, polymer charge density and ionic strength of the solution were varied in order to study the nature of complex formation between latices and polyelectrolyte chains. Recently, special approaches have been proposed for a reliable angular dependence extrapolation of the scattering curves in polydisperse systems.[22−24]

The protein polyelectrolyte complexes[25,26] and micelle polyelectrolyte complexes[27−34] were investigated in detail by focusing on the complex structure as well as on the effect of ionic strength on binding stoichiometry. The structural parameters of the complexes were determined using light scattering measurements. A mechanism of the complexation process was suggested, which explained the stoichiometric complex formation at low and the nonstoichiometric complex formation at high ionic strength.

Some interesting results of light scattering studies in polyelectrolyte complexes were reported by Hara et al.[35] The pronounced influence of the ionic strength of the solution and of the mixing ratio of polyelectrolyte components (heparin-aminoacetalized poly(vinyl alcohol)) on the complex formation was discussed.

Despite a great deal of effort, the general relationship of the mechanism of complex formation is still lacking due to the high complexity of the phenomena. The response of the complex particles to the variation of the experimental conditions is very different depending on the peculiarities of the system investigated.

The present work focuses on the investigation of the mechanism of interaction of oppositely charged polyions and the resulting structure of polyelectrolyte complexes in dilute solution using static and dynamic light scattering and flow birefringence (FB) techniques. Both methods are very sensitive to aggregation, which make them especially effective in analysis of particle structure, size, and shape.

Experimental Section

Well-characterized synthetic flexible polyelectrolytes were used for the complex formation: quaternized poly(vinylpyridinium) (QPVP) as the polycation and poly(sodium styrene)sulfonate (NaPSS) as the polyanion component. QPVP was prepared by quaternization of anionically synthesized poly(2-vinylpyridine) by reaction with benzyl bromide.[36−38] The degree of quaternization of the QPVP sample was calculated from the Br/N ratio, which was determined by elemental analysis and counterion titration. The degree of quaternization of the QPVP was 100%. NaPSS was purchased from Polymer Standard Service, Mainz, Germany, anionically prepared, sulfonated, and characterized by elemental analysis. Molecular weights of the samples were determined by static light scattering experiments: $M_w = 2.0 \times 10^6$ for QPVP and $M_w = 2.0 \times 10^5$ for NaPSS. More details about sample preparation and characterization are described elsewhere.[36−38]

† Dedicated to Prof. Victor N. Tsvetkov, Institute of Macromolecular Compounds, Russian Academy of Sciences, St. Petersburg, Russia, on the occasion of his 87th birthday.

‡ University of Massachusetts.

§ St. Petersburg State University.

⊗ Abstract published in *Advance ACS Abstracts,* August 1, 1997.

S0024-9297(96)01798-6 CCC: $14.00

The polycation (QPVP) and polyanion (NaPSS) were dissolved separately in an appropriate organic solvent *N*-methylformamide (NMFA), spectral grade, with an added 0.01 M of low molecular weight salt KBr. Stock solutions (10^{-3} g/mL) were diluted and mixed directly in the light scattering cells after being filtered through a Milex GS 0.2 μm pore sized filter in order to avoid polymer losses (clusters) on the filter. The polyanion (PA) solution was added to a polycation (PC) solution of the same concentration. The range of investigated concentrations was $c = (10^{-5}-10^{-6})$ g/mL in LS and $c = 2.5 \times 10^{-4}$ g/mL in FB. (FB measurement was not possible at the same concentrations as LS because of the experimental limits of sensitivity.) The molar ratio, m, of the mixed components was defined as

$$m = \frac{n^-}{n^- + n^+} = \left(\frac{V^+}{V^-}\frac{Xm^+}{Xm^-} + 1\right)^{-1} \quad (1)$$

where n^- and n^+ are the number of negative and positive charges on the PA and PC chains, respectively, Xm^- and Xm^+ are the molar concentrations of the PA and PC chains, respectively, and V^- and V^+ are the mixed volumes of the PA and PC solutions, respectively.

The stability of all prepared mixtures was checked by measuring the intensity of scattered light in time with a simultaneous multiangle instrument continuously from 30 min to 4 days after mixing. In the chosen organic solvent no changes in the intensity were monitored. Solutions prepared with water as a solvent (H_2O + 0.01 M KBr) showed a rapid decrease in intensity after 5 h, indicating cluster instability, and consequently, such aqueous solvents were excluded from this investigation. All measurements were taken starting 1 h after mixing.

All experiments were conducted under conditions in which the ionic strength, temperature ($T = 293$ K), total polymer weight concentration, and mixing ratio were controlled.

Light scattering measurements were performed in the range of scattering angle from 25° to 140° with a commercially available spectrometer consisting of an ALV-SP81 goniometer and an ALV-3000 or ALV-5000 correlator. A krypton laser, Spectra Physics, Model 2060, and an ADLAS Nd-YAG-laser (doubled frequency) operating at 647.1 and 532 nm wavelengths were used as light sources. Long time measurements were performed with an ALV-1800 multiangle light scattering instrument ($\lambda = 514.5$ nm).[39] Most of the correlation functions were recorded in the realtime "multi-τ" mode. In dynamic light scattering, the time autocorrelation function of the scattered intensity $g_2(t)$ was measured (homodyne method), which was converted to the scattered electric field autocorrelation function $g_1(t)$ via the Siegert relation

$$g_1(t) = \{[g_2(t) - A]/A\}^{1/2} \quad (2)$$

where A is the experimentally determined baseline. $g_1(t)$ was fitted to a sum of two exponentials, using a SIMPLEX algorithm.

$$g_1(t) = a_1(q)\exp[-t/\tau_1(q)] + a_2(q)\exp[-t/\tau_2(q)] \quad (3)$$

In all cases $g_1(t)$ could almost be described by a single exponential relaxation. A second-order cumulant fit was also applied to all correlation functions. The second cumulant parameter, related to particle polydispersity, increased from $m_2 = 0.1$ to $m_2 = 0.3$ when the mixing ratio approached $m = 0.4$. The reduced scattering intensities, $Kc/R(q)$, were derived according to standard procedures using toluene as the reference. The refractive index increments of polyions in NMFA + 0.01 M KBr were measured on the polarizing interferometer $dn/dc = 0.11$.

FB measurements were carried out by the photoelectric compensation method with phase modulation.[40] The intensity of light passing through the crossed polarizer and analyzer was determined by the combined action of the anisotropic layer in the Couette cell, the compensator, and photoelastic modulator with the slow axis oriented at 45° relative to the analyzer axis. The frequency of modulation was 17 kHz. The elliptical compensator had an optical retardation of $0.0366\ \lambda_0$ at a wavelength of 632.8 nm, which was produced by a He−Ne laser. FB was investigated in a cylindrical apparatus with an inner rotor and a thermostated water jacket. The rotor height along the path of the beam was 3.21 cm, and the width of the rotor-to-stator gap was 0.02 cm.

Intrinsic viscosities were measured by the standard method in capillary Ostwald viscometers with a solvent flow time of 75 s. The solvent viscosity was $\eta_0 = 1.85$ cP.

Experimental Results and Discussion

Light Scattering. Static Light Scattering. The properties of the light scattered by polyelectrolyte mixtures in dilute solutions $c = (1-10) \times 10^{-6}$ g/mL were found to be dependent on the molar ratio, m, of the mixed components.

When polycation or polyanion components in mixed solution are in excess ($m < 0.2$ or $m > 0.6$), the experimental scattering curves have a well-known form according to Zimm's extrapolation (4), which holds for $qR_g \leq 1$,

$$\frac{Kc}{R(\theta)} = \frac{1}{M_w}\left(1 + \frac{1}{3}q^2R_g^{\ 2} + ...\right) \quad (4)$$

Here $q = (4\pi/\lambda)\sin(\theta/2)$ is the scattering vector, λ is the wavelength of the light in the medium, θ is the scattering angle, R_g and M_w are the radius of gyration and molecular weight of the particle, respectively, c is the total polymer concentration, $K = 4\pi^2 n_0^2 (dn/dc)^2/N_A\ \lambda_0^4$ is the optical constant, n_0 is the refractive index of the medium, λ_0 is the wavelength of the primary beam in vacuum, and dn/dc is the refractive index increment of the system.

In the range of $0.2 < m < 0.5$ Zimm plots show a deviation from the linear behavior expected from Gaussian coils (concave upward curves, Figure 1). This upward concavity could be indicative of a spherical structure.

Estimation of the particle's dimension according to eq 4 in the range of $0.03 \leq m \leq 0.2$ and $0.6 \leq m \leq 0.9$ led to $R_g \geq 1000$ Å, which corresponds to the $qR_g > 1$ region. If $qR_g > 1$, light sees the interior of the flexible polymers. The corresponding scattering curves exhibit a power law of q, $I(q) \sim R(q) \sim q^{-d}$ with $d = 1$ for a stretched polymer, $d = 5/3$ for an excluded volume regime, $d = 2$ for a Gaussian chain, and $d = 3$ for a sphere.[41]

The highest values attainable in our experiment are around $qR_g = 8$ (see later Figure 8). At $R_g = 1000$ Å we attain in our experiment $qR_g = 3.3$. This justifies

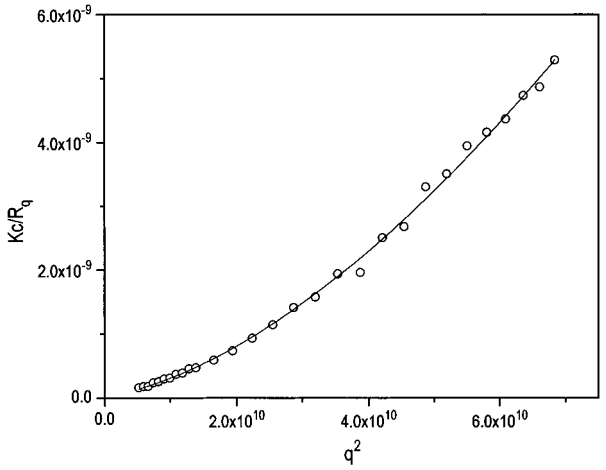

Figure 1. Scattering curve for the polyelectrolyte complex (PEC)(NaPSS/QPVP) at polymer concentration $C = 10^{-5}$g/mL and mixing ratio $m = 0.35$. Experimental points are fitted by eq 5.

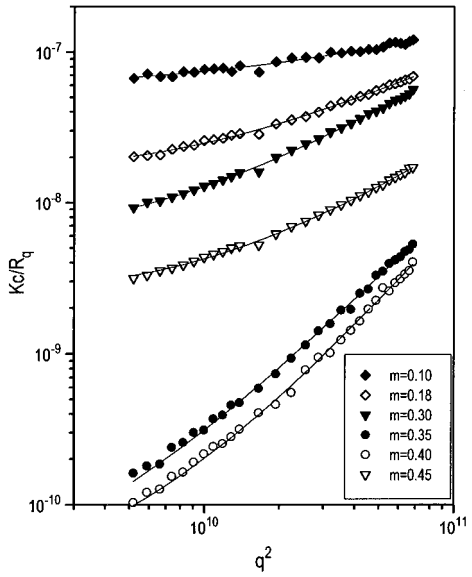

Figure 2. Scattering curves for the PEC (NaPSS/QPVP) at polymer concentration $C = 10^{-5}$ g/mL and different mixing ratios m defined on the figure. Experimental points are fitted according to eq 5. Estimated fractal parameter d: 0.71 (m = 0.1); 1.50 (m = 0.183); 1.94 (m = 0.3); 3.28 (m = 0.35); 3.75 (m = 0.4); 2.24 (m = 0.45).

the use of the Fisher−Burford approach[42] (eq 5) in order to determine the apparent radius of gyration R_g and fractal exponent d of the investigated particles

$$\frac{Kc}{R(\theta)} = \frac{1}{M_w}\left[1 + \frac{2}{3d}q^2 {R_g}^2\right]^{d/2} \qquad (5)$$

According to eq 5 the corresponding scattering curves exhibit power law of q, i.e., $Kc/R(\theta) \sim q^d$, with d being a fractal exponent of the particles. This approach has been applied to studies on fractal colloidal aggregates,[43] wormlike micelles,[44] and polyampholyte chains.[45]

Figure 2 shows the log−log variation $Kc/R(\theta)$ versus q^2 for the system NaPSS/QPVP with different molar ratios. At low mixing ratios (m = 0.10, m = 0.18) normal Zimm-like behavior is observed, while at higher mixing ratios (m > 0.3) stronger nonlinear behavior is observed (also shown in Figure 1 for $m = 0.35$). Values for R_g and d can be estimated from the curves in Figure 2 using eq 5. Values of R_g are plotted versus the mixing ratio m in Figure 3. Apparent radii of gyration R_g show a significant increase from $R_g \sim 1000$ Å at $m = 0.1$ to $R_g \sim 3000$ Å at $m = 0.35-0.4$ with the corresponding increase in the fractal parameter from $d = 0.75$ to $d = 3.75$. At m > 0.4 a rapid asymmetric decrease in R_g and d is observed.

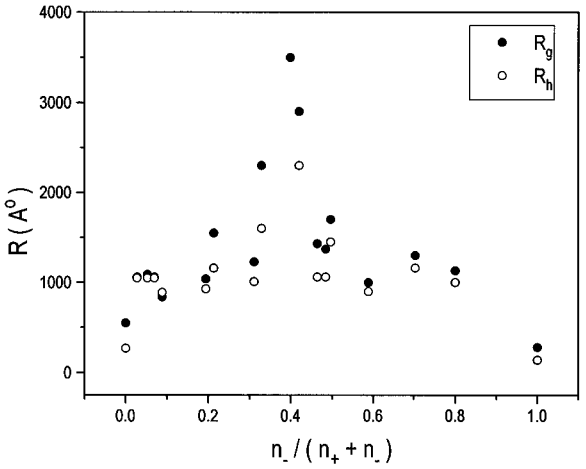

Figure 3. R_g and R_h vs m for the PEC (NaPSS/QPVP). Polymer concentration for both components $C = 10^{-5}$ g/mL.

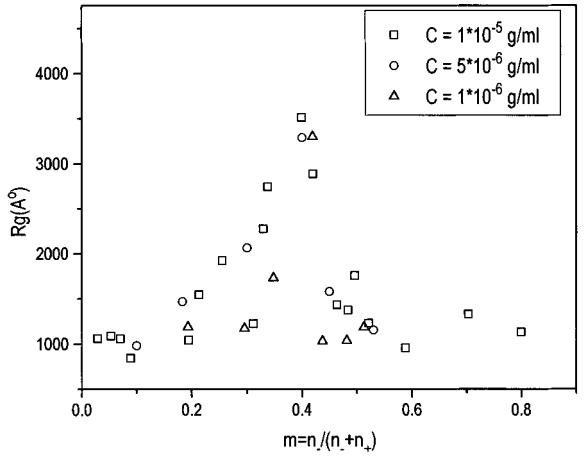

Figure 4. Radius of gyration vs mixing ratio m for the PEC (NaPSS/QPVP) at different polymer concentrations defined on the figure. (Both polyions have equal concentrations.)

This might be interpreted as the process of complex formation of the aggregates with increasing dimensions $R_g \approx 1000-3000$ Å (Figure 3) and with correspondingly changing shape $d \sim 1-3$ (see note to Figure 2). As the clusters grow and R_g increases (when $m \rightarrow 0.4$), the crossover to the power-law behavior occurs at even smaller values of q (Figure 2). Figure 4 shows R_g versus mixing ratios for different concentrations. No dependence on concentration is shown over the range of concentrations investigated $C = 10^{-5}-10^{-6}$.

The extrapolation $Kc/R(q)$ to zero q and c provides an estimate of the weight average molecular weight (eqs 4 and 5). In addition, one can estimate an average polymer density, Φ, within the clusters by assuming a roughly spherical nondrained conformation of the complex. This leads to

$$\Phi = \frac{3M}{4\pi N_A {R_{sph}}^3} \qquad (6)$$

where $R_{sph} = (5/3)^{1/2}R_g \approx 1.29R_g$. Figures 5 and 6 show

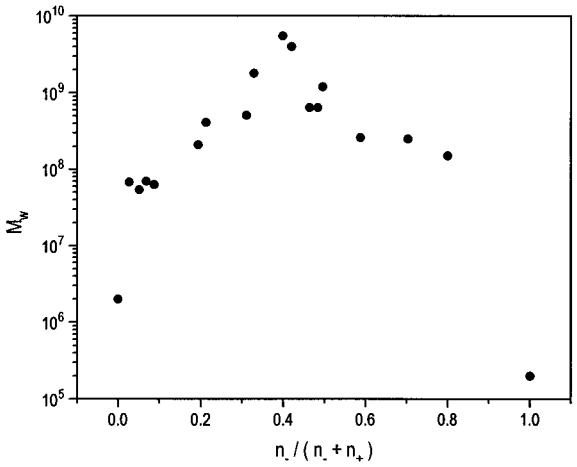

Figure 5. Dependence of M_w on the mixing ratio m for the PEC (NaPSS/QPVP). Polymer concentration for both polyions $C = 10^{-5}$g/mL.

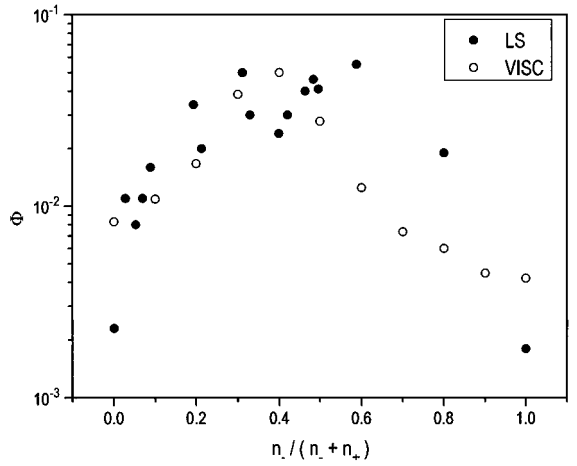

Figure 6. Average polymer density Φ within the PEC (Φ is the volume fraction of polymer inside a hydrodynamically equivalent sphere) vs m.

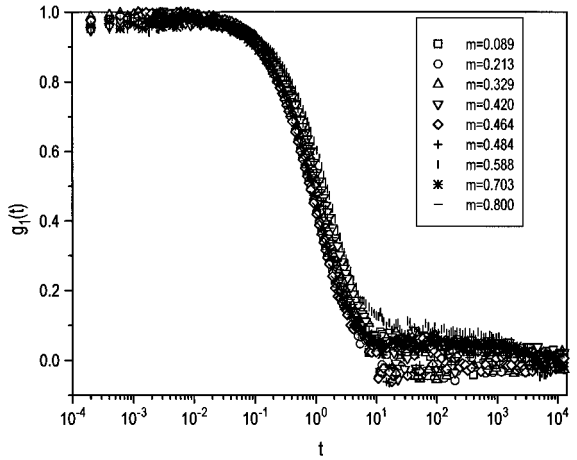

Figure 7. Autocorrelation function $g_1(t)$ for the PEC (NaPSS/QPVP) vs time at different mixing ratios m and at polymer concentration $c = 10^{-5}$ g/mL.

a large increase in molecular weight and polymer density of the clusters at a critical value $m = 0.4$ (gelation process) and sharp decrease in the postgel region.

Dynamic Light Scattering. Autocorrelation functions $g_1(t)$ for polyelectrolyte complexes with different mixing ratios m are presented in Figure 7. No "slow mode" was detected.

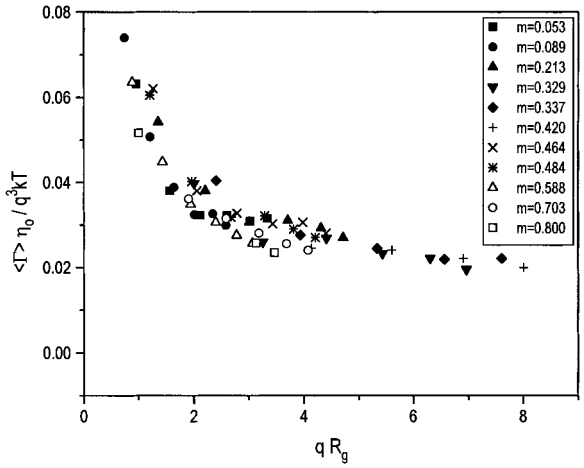

Figure 8. Normalized first cumulant vs qR_g for the PEC (NaPSS/QPVP) at different mixing ratios m defined in the figure.

In the range $qR_g < 1$, i.e., $q^{-1} > R_g$, the autocorrelation function

$$g_1(t) = \int_0^\infty W(g,\Gamma)e^{-\Gamma t}\,d\Gamma \tag{7}$$

is close to a single exponential with a mean decay rate $\langle\Gamma\rangle$ related to the translational diffusion coefficient of the whole cluster D by

$$\langle\Gamma\rangle = Dq^2 \tag{8}$$

$$D = kT/6\pi\eta_0 R_h \tag{9}$$

with k the Boltzmann constant, T the absolute temperature, and R_h the hydrodynamic radius.

In the range $qR_g > 1$ the characteristic scale of fluctuations in q^{-1} becomes smaller than the overall dimensions of R_g, i.e., $q^{-1} < R_g$. This means that relaxation of the fluctuations is due to internal modes of the chains, and $\langle\Gamma\rangle$ is now related to the internal mobility in the cluster, i.e., to the internal diffusion coefficient $D_i \sim q$. Consequently,

$$\langle\Gamma\rangle \sim D_i q^2 \sim q^3 \tag{10}$$

Akcasu et al.[46,47] and Lee et al.[48] developed models for the interpretation of the dynamic light scattering experiment in terms of the first cumulant $\langle\Gamma\rangle$ of the intermediate scattering function. It was found that

$$\langle\Gamma\rangle = A\frac{kT}{\eta_0}q^3 \tag{11}$$

Here A is the prefactor, which is dependent on the quality of the solvent. For solutions in a good solvent $A \approx 0.08$[46,47] and $A \approx 0.045$.[48]

Plotting the angular dependence of the first cumulant normalized with respect to temperature, viscosity, and q^3, i.e., $\langle\Gamma\rangle\eta_0/(q^3kT) = f(q)$, we should observe the decrease in $\langle\Gamma\rangle\eta_0/(q^3kT)$ (when $\langle\Gamma\rangle$ is governed by eqs 8 and 9) and observe saturation in $\langle\Gamma\rangle\eta_0/(q^3kT)$ (when $\langle\Gamma\rangle$ is governed by eqs 10 and 11).

Such plot is shown in Figure 8. With increasing q values more and more of the internal mobility is detected. A well-pronounced plateau indicates self-similarity of the internal relaxation.

The experimental limit at $qR_g \rightarrow \infty$ (Figure 8) is 2 times lower than theoretically predicted.[48] This dis-

crepancy might be reasonable if we take into account the complexity and polydispersity of the system in comparison with theoretical models[48] developed for the single polymer chains. A similar asymptotic decrease of experimental angular dependence of the first cumulant below the theoretical limit was also reported in the literature for several systems.[49,50] The extrapolation of $\langle\Gamma\rangle/q^2$ to zero q according to eqs 8 and 9 leads to the values of the hydrodynamic radius, R_h, that are slightly different from the corresponding R_g values and show a similar dependence versus m (Figure 3).

Comparing experimental results represented in Figures 2−6 we note the following trends. When the polycation or polyanion is in excess ($m < 0.2$ or $m \geq 0.6$, respectively) the complexes formed are stable with dimensions $R_g \approx R_h \approx 1000$ Å.

In the range of $m = 0.3-0.4$ a dramatic increase of R_g, R_h, M_w, and Φ values is observed.

To interpret this finding, we envision the model described in the figure below

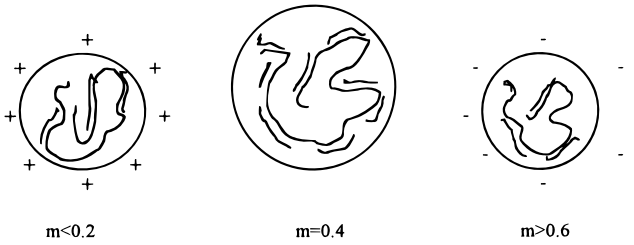

One can consider the polyelectrolyte complex (PEC) in a manner analogous to block copolymers containing sequences of "MFA-phobic" double-stranded and "MFA-philic" single-stranded segments. When an excess of free polyions (+ or −) is present ($m \leq 0.2$ or $m \geq 0.6$), these "MFA-philic" polyions stabilize and screen "MFA-phobic" complex particles. In the case of less than an excess of free polyions ($m = 0.4$) these complex particles tend to interact and grow (no screening effect), which is reflected in the significant increase of averaged dimensions, molecular weight, and polymer density. In other words, at $m \rightarrow 0.4$, an increased number of "MFA-phobic" areas are formed in the growing PEC and the latter tends to grow and precipitate (fluctuational network formation).

The unanswered question is, why should these inter-polyelectrolyte interactions show nonstoichiometric behavior ($m_c = 0.4$), i.e., the strongest interaction occurs at 60% of polycation and 40% of polyanion component? One reason might be the hindrance of rotation (bulky side groups) in the polycation chains. This reason, however, cannot be accepted without some doubt, because the hindrance of rotation in PC chains should be considered as relatively high in order to satisfy $m_c = 0.4$ (each second charge in the PC chain must not be reached for PA interaction). The second reason may reflect an incomplete (not 100%) quaternization of QPVP samples.

It is possible that, at low and high mixing ratios m, there is an excess of free polyions in addition to the clusters. The decoupling of these individual contributions is not possible in the experiment because of its physical origin: the average intensity of all scattering species is measured. The sample can be more selectively probed at different length scales by application of an external orienting field. This technique is explored in the next section.

Flow Birefringence. In the FB method anisotropic and anisometric particles are oriented in the external shear field. The macroscopic anisotropy in the solution of rigid spheroids is determined[51] by the value of birefringence

$$\Delta n = 2\pi N(\gamma_1 - \gamma_2)f(\sigma,p)/n_s \qquad (12)$$

and orientation (extinction) angle, i.e., the angle between the optical axis of the solution and the flow direction.

$$\cot 2\varphi_m = \varphi(\sigma,p) \qquad (13)$$

Here f(σ,p) and $\varphi(\sigma,p)$ are orientation factors tabulated in ref 52 as functions of shape asymmetry $p = L/d$ ($p = \infty$ for a thin rod, $p = 1$ for a sphere, $p = 0$ for a thin disk) and orientation parameter $\sigma = g/D_r = \eta_0 W/kT$, g is the gradient of the flow rate, D_r is the rotational diffusion (or W is rotational friction) coefficient of the spheroid about the short axis, $(\gamma_1 - \gamma_2)$ is the optical anisotropy of the spheroid, N is the number of the particles in the unit volume, and n_s is the refractive index of the solvent.

For small $\sigma < 1.5$ we have the power series

$$\Delta n = \frac{2\pi N}{n_s}(\gamma_1 - \gamma_2)\frac{\sigma b}{15}\left[1 - \frac{\sigma}{72}\left(1 + \frac{6b^2}{35}\right) + ...\right] \qquad (14)$$

$$\varphi_m = \frac{\pi}{4} - \frac{\sigma}{12}\left[1 - \frac{\sigma}{108}\left(1 + \frac{24}{35}b^2\right) + ...\right] \qquad (15)$$

where $b = (p^2 - 1)/(p^2 + 1)$ for a prolate ellipsoid.

With increasing $\sigma = g/D_r$, the birefringence Δn increases more slowly than σ and the corresponding curve bends toward the σ (or g) axis (negative departure from proportionality), and so, the smaller D_r (larger particle size) the more rapidly it approaches saturation. The extinction angle φ_m starts at 45° and decreases more rapidly for the particles with smaller D_r (larger size) but in any case approaches the common limit $\varphi_m = 0$ for $\sigma \rightarrow \infty$. It means that large particles ($W \rightarrow \infty$) are oriented at lower gradients, g, i.e., reach full orientation along flow direction $\varphi_m = 0$, and full saturation in the birefringence f(σ,p) = 1. Small particles ($W \rightarrow 0$) in the same range of velocity gradients may still not reach full orientation, and birefringence shows a linear dependence on σ.

The hydrodynamic and optical properties of polyelectrolyte mixtures in FB were found to be strongly dependent on the molar ratio. For PC ($m = 0$) and PA ($m = 1$) solutions, the orientation angle φ_m was measured to be close to 45°. Corresponding relaxation times $\tau = \lim_{g\rightarrow 0} \tan[2(\pi/4 - \varphi_m)/g]$ are $\tau = 10^{-4}$ s for PC and $\tau = 2 \times 10^{-5}$ s for PA. Δn values are linear functions of the gradient of the shear rate, g, in accordance with molecular dispersal effects of single polyions (Figure 9). The values of shear optical coefficients $\Delta n/\Delta S = \Delta n/g(\eta - \eta_0)$ (η and η_0 are the viscosities of the solution and the solvent, respectively, $\Delta S = g(\eta - \eta_0)$ is the shear stress) are large in magnitude and negative in sign: $\Delta n/\Delta S = -421 \times 10^{-10}$ cm s^2 g^{-1} for PC and $\Delta n/\Delta S = -617 \times 10^{-10}$ cm s^2 g^{-1} for PA. This is due to highly anisotropic pyrimidine (for PC) and styrene (for PA) cycles oriented normal to the chain direction. $\Delta n/\Delta S$ values are close to those found previously for similar flexible polyelectrolytes in solutions with low ionic strength.[51, 53−55]

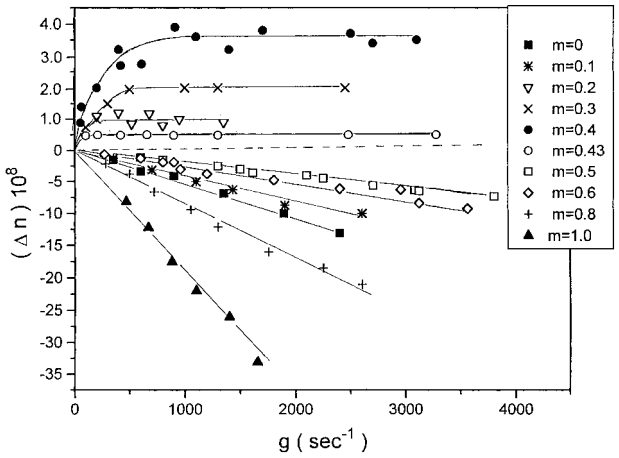

Figure 9. Value of the flow birefringence Δn vs gradient of the flow rate, g, for the PEC at polymer concentration $c = 2.5 \times 10^{-4}$ g/mL and different mixing ratios m defined on the figure.

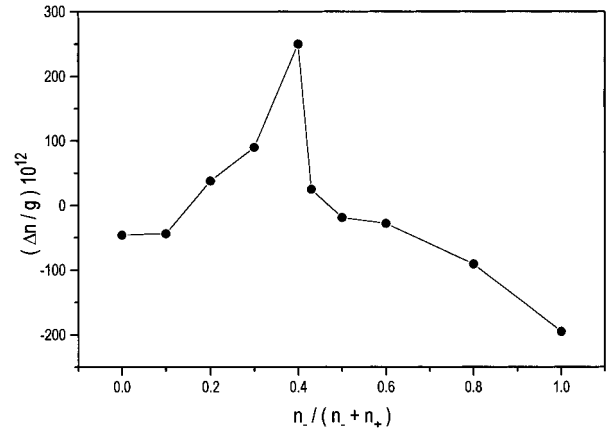

Figure 10. Initial slopes $\Delta n/g$ of the dependences $\Delta n = f(g)$ presented in Figure 9 vs mixing ratio m. The asymmetric decrease in postgel region similar to the ones in Figure 3 is clearly observed.

Experimental curves $\Delta n = f(g)$ (Figure 9) for **mixed** solutions $0 < m < 1$ differ not only in character (linear or with saturation) but also in sign. These changes show that in a multicomponent system (clusters, single chains, and solvent) the orientations (relaxations) of the clusters and of single polyions are essentially different.

Solutions at $0 < m \leq 0.1$ and $0.5 \leq m < 1$ (Figure 9) exhibit negative values of the linear FB, $\Delta n(g)$, and orientation angle φ_m is close to $\pi/4$. This linear effect is caused mainly by the intrinsic FB, Δn_{int}, of free single polyions that are present in solution in excess and consequently could not react with oppositely charged polyions. The initial slope, $\Delta n/g$, of $\Delta n = f(g)$ dependence is related to the number of particles, N, in solution (see eqs 12 and 14). Therefore, the $\Delta n/g$ value produces a qualitative measure of the decrease of the number of free polyions, N, per unit volume in mixed solutions at $m \rightarrow 0.4$ (Figure 10).

Solutions at $0.2 \leq m \leq 0.4$ exhibit positive nonlinear FB $\Delta n(g)$ with full saturation (Figure 9). This effect is caused mainly by the positive macroform effect, Δn_{form}, of the clusters with large dimensions. Initial slopes, $\Delta n/g$, are rapidly increased as one approaches $m = 0.4$, showing the increase of the number of aggregates (Figure 10). The range of velocity gradients $g = (50-4500)$ s^{-1} was too high to monitor the decrease in φ_m from 45° to 0° and orientation angle at all g was measured to be close to zero.

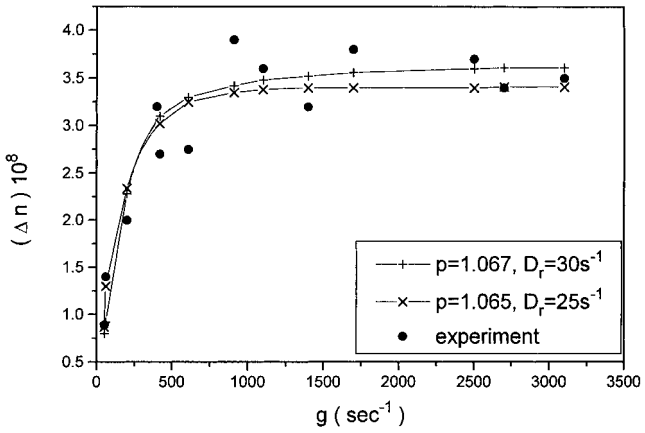

Figure 11. Value of the flow birefringence Δn vs gradiennt of the flow rate, g, for the PEC at $m = 0.4$: (circles) experimental points; (lines) theoretical curves according to eq 18.

The complex is modeled as a rigid solid spheroidal particle consisting of polyelectrolyte molecules with an average refractive index, n, differing from that of the solvent, n_s, and surrounded by continuous solvent media. Assuming that optical anisotropy of the complex particle is caused in the first approximation only by form effect, we have[51,53,54]

$$(\gamma_1 - \gamma_2) \approx (\gamma_1 - \gamma_2)_{form} \equiv \frac{(n^2 - n_s^2)(L_1 - L_2)\nu}{n_s^2\left(4\pi + \frac{n^2 - n_s^2}{n_s^2}L_1\right)\left(4\pi + \frac{n^2 - n_s^2}{n_s^2}L_2\right)} \quad (16)$$

We also take into account that $N\nu = c/\rho$ where ν is the volume of the solid complex particle, N is the number of clusters per unit volume, ρ is the density of dry polymer, c is the concentration of polyions in g/mL; $n^2 - n_s^2 \approx 2n_s\rho\ dn/dc$.[51,53]

The functions of shape asymmetry in eq 16 are expressed as[51,53]

$$L_1 = \frac{4\pi}{3}(1 - 2e) \qquad L_2 = \frac{4\pi}{3}(1 + e)$$

$$e = \frac{1}{4(p^2 - 1)}\left[2p^2 + 4 - \frac{3p}{\sqrt{p^2 - 1}}\ln\frac{p + \sqrt{p^2 - 1}}{p - \sqrt{p^2 - 1}}\right] \quad (17)$$

Then the final expression for Δn_{form} is

$$\Delta n_{form} = \frac{2\pi N}{n_s}(\gamma_1 - \gamma_2)_{form} f(\sigma,p) = \frac{2\pi c(2n_s\rho\ dn/dc)^2 e}{\rho n_s\left[1 + \frac{2n_s\rho\ dn/dc(1 - 2e)}{3n_s^2}\right]\left[1 + \frac{2n_s\rho\ dn/dc(1 + e)}{3n_s^2}\right]} f(\sigma,p) \quad (18)$$

Experimental points $\Delta n = f(g)$ (Figure 11) were approximated according to least squares by theoretical functions (*17*), (*18*)] using the following values $dn/dc = 0.1$; $n_s = 1.4319$; $\rho = 1.5$; $c = 2.5 \times 10^{-4}$ g/mL. The shape asymmetry, $p = 1.07$, and rotational diffusion coefficient, $D_r = 26\ s^{-1}$, of the clusters were determined at $m = 0.4$. The shape asymmetry parameter, $p = 1.07$, suggests that clusters have a very low degree of asphericity (roughly spherical). Using spherical approxima-

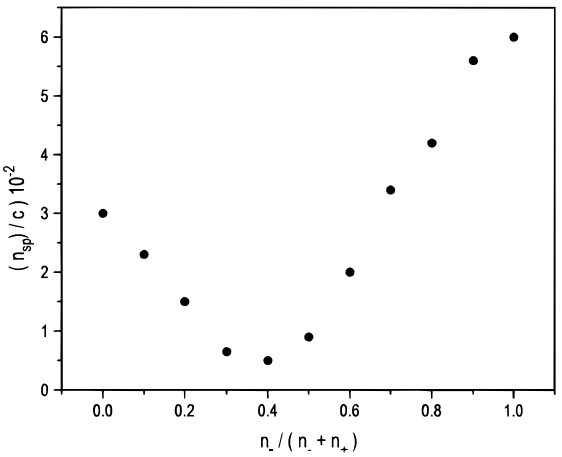

Figure 12. Specific viscosity η_{sp}/c vs mixing ratio, m, for the PEC at polymer concentrations $c = 2.5 \times 10^{-4}$g/mL.

tion, average dimensions of the clusters at $m = 0.4$ were estimated, $R = (kT/8\pi\eta_0 D_r)^{1/3} = 1500$ Å, half that from LS $R_g \approx R_h \approx 3000$ Å. This discrepancy might be due to the simplicity of the hydrodynamic model (rigid spheroid) used in FB. One cannot exclude the possibility that clusters are spheres at rest and are slightly deformed in the flow.

Viscosity. Figure 12 reveals a nonlinear dependence of the reduced viscosity η_{sp}/c of the solutions on m. The dependence has a well-pronounced minimum at $m = 0.4$. The viscosity of the solution of the particles is a measure of the frictional energy loss when the particles are rotated in the flow. Therefore the decrease in η_{sp}/c approaching $m = 0.4$ might be attributed to the change in particle conformation from anisometric extended conformations of single polyions at $m = 0$ and $m = 1$ to more spherical conformations of the clusters at $m \rightarrow 0.4$.

The intrinsic viscosity of the cluster $[\eta]$ is a measure of the inverse polymer density inside a hydrodynamically equivalent sphere

$$[\eta] = 2.5/\Phi \qquad (19)$$

where Φ is given by eq 6. Assuming roughly that $\eta_{sp}/c \approx [\eta]$ at $c = 2.5 \times 10^{-4}$ g/mL, we estimated Φ (Figure 6). Φ values are close to the ones received from LS (Figure 6), which confirms spherical conformations of the clusters at $m \rightarrow 0.4$. Discrepancies at low and high mixing ratios show inadequacy of the spherical model for single polyions with elongated conformations.

Thus, SLS, DLS, FB, and viscometry confirm the polyelectrolyte complex formation in the NaPSS/QPVP system. The combination of both polymer and electrolyte properties results in the complexity of the system investigated. However some general trends can be extracted.

Conclusions

1. The polyelectrolyte NaPSS/QPVP complexes are formed in dilute solutions (10^{-6} g/mL $\leq c \leq 10^{-4}$ g/mL in NMFA + 0.01 M KBr) at all molar ratios $0.03 \leq m \leq 0.9$ investigated. This formation of complexes is associated with a drastic increase of molecular weight, average polymer density, and average dimensions, effective relaxation time, and form optical anisotropy in flow birefringence in comparison with the same molecular characteristics for the single chains.

2. Angular distributions of the scattered intensity suggest a crossover from a normal behavior at the low q range to an intermediate regime characterized by a power law. The corresponding increase of the molecular characteristics of the clusters M_w, R_g, R_h, average polymer density, and fractal parameter is observed when the molar ratio approached $m = 0.4$.

3. With an excess of polycations or polyanions ($0.03 < m < 0.2$ and $0.5 < m < 0.9$, respectively) the complexes are stable and have a roughly spherical shape with dimensions $R_g \approx R_h \approx 1000$ Å irrespective of the concentration of the polyions. The excess of free polyions form a screening hydrophilic shell and stabilize the complexes.

4. When only a small excess of free polyions (+ or −) is present, these complexes tend to interact and grow in size and number. The molar ratio $m = 0.4$ may be defined as a gel point for the system (fluctuational gel network formation). At the gel point complexes have average dimensions $R_g \approx R_h \approx 3000$ Å according to LS and $R \approx 1500$ Å according to FB data. Direct determination of shape asymmetry from FB data shows low asphericity (axial ratio) $p = 1.07$ of generated clusters.

5. The cluster model consisting of polyion molecules and immobilized solvent (hydrodynamically nondrained particle) with roughly spherical conformation can be considered as an adequate one.

Acknowledgment. The scientific idea for this work was proposed by Professor Manfred Schmidt, Johannes Gutenberg University, Mainz. The authors are also grateful to him for providing the samples and equipment for the light scatteing experiments at the University of Bayreuth, Gemany. The authors also acknowledge the helpful comments on the paper, provided by Professor Gerald Fuller at Stanford University, California.

References and Notes

(1) Kabanov, V. *Makromol. Chem., Macromol. Symp.* **1991**, *48/49*, 425−426.
(2) Isumrudov, V.; Zezin, A.; Kabanov, V. *Usp. Khim.* **1991**, *60* (7), 1570−1595.
(3) Zezin, A.; Isumrudov, V.; Kabanov, V. In *Frontiers of Macromolecular Science*; Saegusa, T., Migashimura, T., Abe, A., Eds.; Blackwell Scientific Publication: Glasgow, 1989; Vol. 219, p 225.
(4) Kabanov, V.; Zezin, A. *Pure Appl. Chem.* **1984**, *56* (3), 343.
(5) Bixler, H. J.; Michaels, A. S. Polyelectrolyte Complexes In *Encycl. Chem. Technol.* **1968**, *16*, 117.
(6) Tsuchida, E.; Abe, K. *Adv. Polym. Sci.* **1982**, *45*, 1130.
(7) Kabanov, V.; Zezin, A.; Mustafaev, M.; Kasaikin, U. *Polym. Amines Amm. Salts* (IUPAC 1979, Chent); Pergamon Press Ltd.: Oxford, U.K., 1980; pp 173−192.
(8) Zezin, A.; Kabanov, V. *Usp. Khim.* **1982**, *51* (9), 1447.
(9) Kabanov, V. A.; Zezin, A. B.; Isumrudov, V. A.; et al., *Macromol. Chem. Suppl.* **1985**, *13*, 137.
(10) Bakeev, K. N.; Isumrudov, V. A.; Zezin, A. B.; Kabanov, V. A. *Dokl. Akad. Nauk SSSR* **1988**, *299* (6), 1405−1408.
(11) Bakeev, K. N.; Isumrudov, V. A.; Kuchanov, S. I.; Zezin, A. B.; Kabanov, V. A. *Dokl. Akad. Nauk SSSR* **1988**, *300* (1), 132−135.
(12) Astaf'eva, I. V.; Kalyuzknaya, R. I.; Khul'chayev, Kh. Kh.; Tatarova, L. A.; Yermakova, T. J.; Zezin, A. B.; Kabanov, V. A. *Polym. Sci. SSSR* **1991**, *33* (2), 216−223.
(13) Bakeev, K. N.; Isumrudov, V. A.; Kuchanov, S. I.; Zezin, A. B.; Kabanov, V. A. *Macromolecules* **1992**, *25*, 4249−4254.
(14) Kabanov, V. A.; Giriakova, M. V.; Kargov, S. I.; Zezin, A. B.; Isumrudov, V. A. *Dokl. Akad. Nauk SSSR* **1993**, *329* (1), 66−70.
(15) Vishalakshi, B.; Ghosh, S.; Kalpagam, V. *Polymer* **1993**, *34* (15), 3270−3275.
(16) Philipp, B.; Linow, K.-J.; Dautzenberg, H. *Acta Chim. Hung.* **1984**, *117* (1), 67−83.
(17) Philipp, B.; Dawydoff, W.; Linow, K.-J. *Z. Chem.* **1982**, *22* (1), 1−13.
(18) Dautzenberg, H.; Linow, K.-J.; Philipp, B. *Acta Polym.* **1982**, *33* (11), 619−625.
(19) Dautzenberg, H.; Linow, K.-J.; Philipp, B. *Plaste Kautschuk* **1982**, *29* (11), 631−634.

(20) Kötz, J.; Linow, K.-J.; Philipp, B.; Dautzenberg, H. *Acta Polym.* **1986**, *37*, 108−112.
(21) Philipp, B.; Dautzenberg, H.; Linow, K. -J.; Kötz, J.; Dawydoff, W. *Prog. Polym. Sci.* **1989**, *14*, 19.
(22) Dautzenberg, H.; Rother, G. *J. Polym. Sci., Part B: Polym. Phys. Ed.* **1988**, *26*, 353.
(23) Dautzenberg, H.; Rother, G. *Makromol. Chem., Macromol. Symp.* **1992**, *61*, 94.
(24) Dautzenberg, H.; Rother, G.; Hartmann, J. In *Macroion Characterization*; Schmitz, K. S., Ed.; American Chemical Society: Washington, DC, 1994; Chapter 16, p 210.
(25) Xia, J.; Dubin, P. L.; Ahmed, L. S.; Kokufuta, E. In *Macroion Characterization*; Schmitz, K. S., Ed.; American Chemical Society: Washington, DC, 1994; Chapter 17, pp 224−242.
(26) Dubin, P.; Ross, T. D.; Sharma, I.; Yegerlehner, B. In *Ordered Media in Chemical Separations*; Minz, W. L., Armstrong, D. W., Eds.; American Chemical Society: Washington, DC, 1987; Chapter 8.
(27) Dubin, P. L.; The, S. S.; Can, L. M.; Chew, Cn. H. *Macromolecules* **1990**, *23*, 2500−2506.
(28) Dubin, P. L.; Oteri, R. J. *Colloid Interface Sci.* **1983**, *95*, 453.
(29) Dubin, P. L.; Davis, D. D. *Macromolecules* **1984**, *17*, 1294.
(30) Dubin, P. L.; Davis, D. D. *Colloid Surf.* **1985**, *13*, 113.
(31) Dubin, P. L.; Rigsbee, D. R.; McQuigg, D. W. *J. Colloid Interface Sci.* **1985**, *105*, 509.
(32) Dubin, P. L.; Rigsbee, D. R.; Fallon, M. A.; Gan, L. M. *Macromolecules* **1988**, *21*, 2555.
(33) Dubin, P. L.; The, S. S.; McQuigg, D. W.; Gan, L. M.; Chew, C. H. *Langmuir* **1989**, *5*, 89.
(34) Dubin, P. L.; Gan, L. M.; Chew, C. H. *J. Colloid Interface Sci.* **1989**, *128*, 566.
(35) Hara, M.; Nakajima, A. *J. Polym. Sci., Part B* **1989**, *27*, 1043−1056.
(36) Förster, S.; Schmidt, M.; Antonietti, M. *Polymer* **1990**, *31*, 781.
(37) Förster, S. Ph.D. Thesis, Mainz, Germany, 1991.
(38) Förster, S.; Schmidt, M.; Antonietti, M. *J. Phys. Chem.* **1992**, *96*, 4008.
(39) Wintermantel, M.; Schmidt, M.; Tsukahara, Y.; Kajiwara, K.; Kohjiya, S. *Macromol. Rapid Commun.* **1994**, *15*, 279−284.
(40) Pogodina, N. V. *J. Polym. Sci., Part B.* **1993**, *31*, 795.
(41) De Gennes, P. G. *Scaling Concepts in Polymer Physics*; Cornell University Press: Ithaca, NY, 1979.
(42) Fisher, M.; Burford, R. *Phys. Rev.* **1967**, *156* (2), 583.
(43) Dietler, G.; Aubert, C.; Cannell, S. D.; Wiltzius, P. *Phys. Rev. Lett.* **1986**, *57*, 3117.
(44) Appell, J; Porte, G. *Europhys. Lett.* **1990**, *12*, 185.
(45) Skouri, M.; Munch, J. P.; Candau, S. J.; Neyret, S.; Candau, F. *Macromolecules* **1994**, *27*, 69−76.
(46) Benmouna, M.; Akcasu, A. Z. *Macromolecules* **1987**, *11*, 1187.
(47) Akcasu, A. Z.; Han, C. C. *Macromolecules* **1981**, *14*, 1090.
(48) Lee, A.; Baldwin, P. R.; Dono, Y. *Phys. Rev.* **1984**, *A30*, 968.
(49) Trappe, V.; Burchard, W. *Polym. Prepr. (Am. Chem. Soc., Div. Polym. Chem.)* **1994**, *35* (1), 179.
(50) Lodge, T. P.; Han, Ch. C.; Akcasu, A. Z. *Macromolecules* **1983**, *16*, 1180−1183.
(51) Tsvetkov, V. N. *Rigid Chain Polymers*, Plenum: New York, 1989.
(52) Scheraga, H. A.; Edsall, J. T.; Gadd, J. O. *J. Chem. Phys.* **1951**, *19*, 1101.
(53) Tsvetkov, V. N.; Eskin, V. E.; Frenkel, S. J. *Struktura Macromolecul v Rastvorakh*, Nauka: Moscow, 1964.
(54) Tsvetkov, V. N. In *Newer Methods of Polymer Characterization*; Ke, B., Ed.; Interscience: New York, 1964; p 563.
(55) Peterlin, A.; Munk, P.; In *Physical Methods of Chemistry*; Weissberger, A., Rossiter, B., Eds.; Interscience: New York, 1972; p 271.

MA9617983